MEASUREMENTS OF DENSITY TURBULENCE WITH FIR LASER SCATTERING IN THE ASDEX TOKAMAK

G. Dodel and E. Holzhauer
Institut für Plasmaforschung, Universität Stuttgart, Stuttgart, FRG

H. Niedermeyer, K. McCormick, ASDEX-, ICRH-, NI- and Pellet-Teams
Max-Planck-Institut für Plasmaphysik, EURATOM Association, Garching, FRG

Previous measurements of density turbulence in ASDEX [1], [2] were limited to a wavenumber range $k_\perp > 5\ cm^{-1}$ and to distances $\lesssim 21$ cm of the measuring chords from the plasma centre. After modification of the scattering system the important range of lower $k_\perp$ and the region near the separatrix are now accessible. First results of the investigations are presented.

Scattering system:

The scattering system using a 100 mW, 119 µm CW CH_3OH laser and homodyne detection with a Schottky diode is shown in a schematic view in Fig.1.

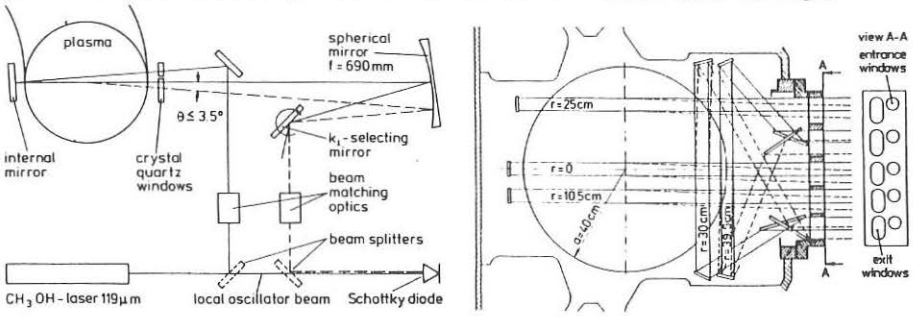

Fig. 1 Left: Schematic of the optical setup. Right: Poloidal section of ASDEX showing the beam paths inside the plasma vessel for the different chords and the window array. The scattered beams are indicated schematically by dashed lines.

The parameters of the scattering experiment are as follows:
beam waist in the plasma: $w_o = 1.6$ cm
wavenumber range: $2.5\ cm^{-1} \lesssim k_\perp < 25\ cm^{-1}$
wavenumber resolution: $\pm 1.25\ cm^{-1}$
spatial resolution: ± 1.6 cm perpendicular to beam, chord averaged along line of sight
Accessible chords (distance measured from plasma center):
horizontal: 0 cm, 10.5 cm, 25 cm; vertical: 33 cm, 39.5 cm
frequency analysis: spectrum analyser with fixed channels and continuous frequency sweeps in plateau phases
wavenumber scan: possible within one plasma shot.
spatial scan: different measuring chords can be chosen from shot to shot.

Ohmic discharges: Evidence for driftwave nature of the turbulence.

The following findings on ASDEX are consistent with the assumption of density gradient driven driftwave turbulence:

a) The rms value of the frequency integrated scattered power scales linearly with the mean electron density if the relative density profiles remain fairly similar. This was established for $n_e < 5 \times 10^{13}$ cm^{-3} (where $\tau_E \propto n_e$ in ASDEX) in the important $k_\perp$ range and in different chords.

b) In the central chord which sees primarily poloidally propagating fluctuations a maximum of the scattered power is observed around ~100 kHz in the dominant $k_\perp$ range. This is on the order of the diamagnetic drift frequency evaluated in the gradient region of the discharge. In the outer vertical chord which sees predominantly radially propagating fluctuations the frequency spectra are significantly narrower (Fig. 2).

c) The maximum of the frequency integrated $k_\perp$ spectrum shifts towards lower $k_\perp$ with increasing T_e (Fig. 3). A value $k_\perp^{max} \cdot \rho_s \approx 0.3$ is inferred from the "cold" shots in Fig. 3. It should be kept in mind, however, that the shape of $P_s(k_\perp)$ and the shape of the fluctuation spectrum $n_e(k_\perp)$ are not identical. The latter results from an integration over all spatial Fourier components while $P_s(k_\perp)$ contains only those components which are selected by the scattering geometry.

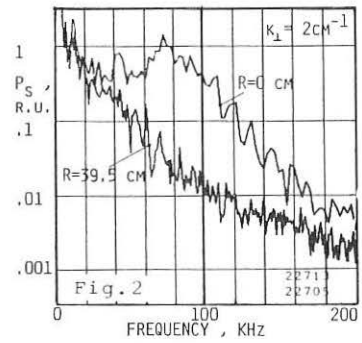

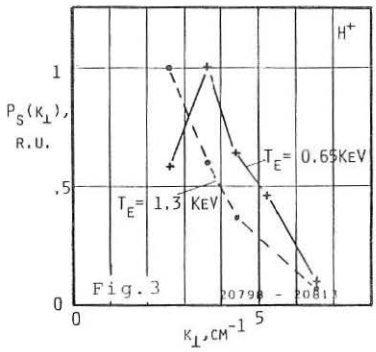

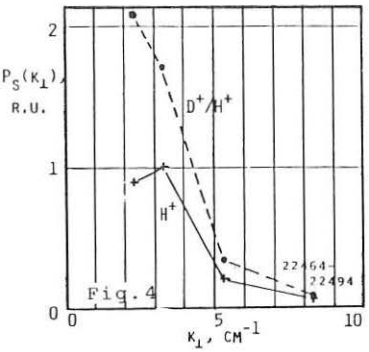

Fig.2: Frequency spectra of scattered power in the central horizontal chord and outer vertical chord (D^+ plasma)

Fig.3: Wavenumber spectra in "hot" and "cold" ohmic hydrogen plasmas. The densities in the center are 1.75×10^{13} cm^{-3} and 4.8×10^{13} cm^{-3}, respectively. Signals are normalized to maximum value. Chord 10.5 cm.

Fig.4: Change of wavenumber spectra with gas filling. Note: Same vertical scale for both curves.

d) The maximum of the frequency integrated $k_\perp$ spectrum shifts towards lower $k_\perp$ and its value increases when the gas filling is changed from pure hydrogen to a ≈1:1 mixture of hydrogen and deuterium at constant electron density (Fig. 4).
e) The frequency and wavenumber integrated scattered power decreases with increasing toroidal magnetic field at constant plasma current.

A detailed analysis is beyond the scope of this summary. It should be noted that unambiguous experimental tests of theoretical models for drift wave turbulence would require pure one-parameter scans which in general are difficult to realize.

L-phase with neutral beam injection (NI):

NI heating produces complex changes of the density turbulence. A dramatic broadening of the frequency spectra with respect to the ohmic phase occurs as is illustrated in Fig. 5. The temporal development of the frequency integrated scattering signal was recorded at the transition from an ohmic to an L-phase, the density profiles remaining essentially unchanged (Fig. 6). The $k_\perp$ spectrum is shifted towards longer wavelengths with NI, and the time behaviour is different for different $k_\perp$. It is an open question wether the change in the spectra is solely due to the increase in T_e or due to a change in nature of the turbulence induced by NI.
As can be seen in Fig. 6 sawtooth activity during NI strongly affects the scattering signals at low $k_\perp$. A clear difference in arrival time and shape of sawteeth on the scattering signals is observed in the different chords (not shown in the figure).

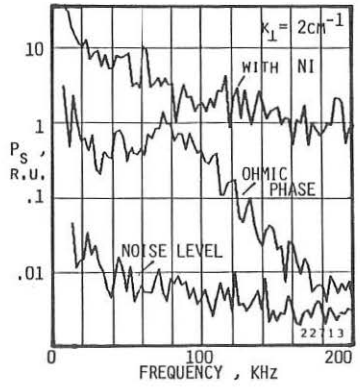

Fig.5: Change of frequency spectra with NI-heating (L-shot; chord 0 cm)

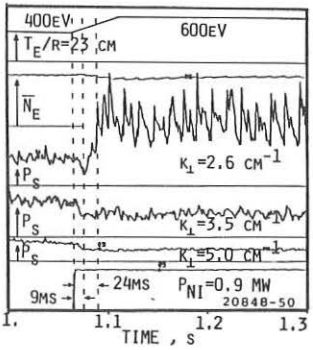

Fig.6: Change of frequency integrated scattering signals for different $k_\perp$ in a series of identical L-shots.

Transition from the L into the burst-free H-phase.

By shifting the horizontal plasma position by a few cm the region inside and outside the separatrix can be scanned with the outer vertical chord. In a series of L-H transitions the behaviour of the fluctuations was investigated at distances of ~0.5 cm outside and ~1 cm inside the separatrix. In both cases the scattering signals decrease sharply at the time of the transition (Fig. 7). This behaviour cannot be explained by a drop in density and/or decrease in the density gradient length, as can be seen from Fig. 8. It shows the density profiles obtained from the Li beam probe before and after the transition as well as the position and radial extent of the FIR laser beam with respect to the separatrix radius r_s.

Further investigations are necessary in order to obtain a conclusive picture of the fluctuation behaviour at the L-H transition.

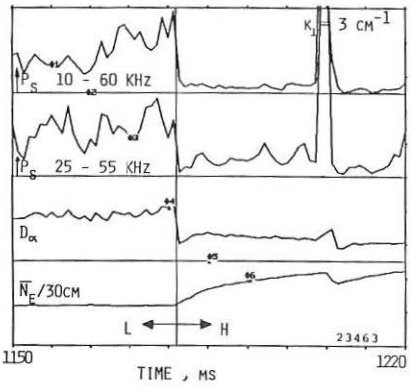

Fig.7: Density fluctuation signals measured close to the separatrix in different frequency channels at the transition from an L-phase into a burstfree H-phase (Outer vertical chord; lower traces: D_α monitor and line electron density).

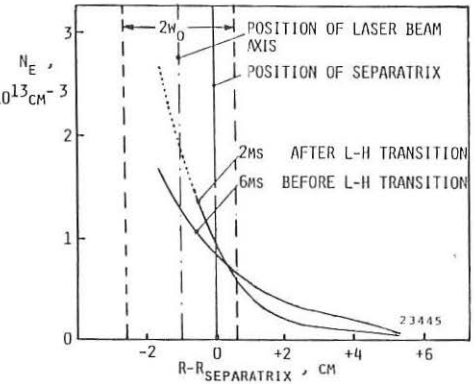

Fig.8: Electron density profiles in the separatrix region before and shortly after the L-H transition. The position and width ($1/e^2$ of intensity) of the laser beam relative to the separatrix are marked with vertical lines.

References

[1] G. Dodel, E. Holzhauer, J. Massig, J. Gernhardt, ASDEX-, ICRH-, LH-, NI- and Pellet Teams, 14th European Conference on Controlled Fusion and Plasma Physics, Madrid, June 1987, Europhys. Conf. Abstr. 11D, I, p. 249

[2] G. Dodel, E. Holzhauer, ASDEX- and NI-Teams, 3rd Int. Symp. on Laser-Aided Plasma Diagnostics, Los Angeles, Oct. 1987, Proceedings p. 146.